ACS OMEGA

http://pubs.acs.org/journal/acsodf

Article

Flux Crystal Growth, Crystal Structure, and Magnetic Properties of a Ternary Chromium Disulfide $Ba_9Cr_4S_{19}$ with Unusual Cr_4S_{15} Tetramer Units

Hong Yan, Yoshitaka Matsushita, Akira Chikamatsu, Tetsuya Hasegawa, Kazunari Yamaura, and Yoshihiro Tsujimoto*

Cite This: *ACS Omega* 2021, 6, 6842−6847

Read Online

ACCESS | Metrics & More | Article Recommendations | Supporting Information

ABSTRACT: A new ternary chromium disulfide, $Ba_9Cr_4S_{19}$, has been grown out of $BaCl_2$ molten salt. Single-crystal structure analysis revealed that it crystallizes in the centrosymmetric space group $C2/c$ with lattice parameters: a = 12.795(3) Å, b = 11.3269(2) Å, c = 23.2057(6) Å, β = 104.041(3)°, and Z = 4. $Ba_9Cr_4S_{19}$ comprises four face-sharing Cr-centered octahedra with disulfide ions occupying sites on each terminal face. The resulting Cr_4S_{15} tetramer units are isolated by nonmagnetic Ba-centered polyhedra in the ab plane and barium disulfide ($=Ba_4(S_2)_2$) layers along the c-axis. Following the structure analysis, the title compound should be expressed as $[Ba^{2+}]_9[Cr^{3+}]_4[(S_2)^{2-}]_4[S^{2-}]_{11}$, which is also consistent with Cr2p X-ray photoemission spectra showing trivalent states of the Cr atoms. The unique Cr-based zero-dimensional structure with the formation of these disulfide ions can be achieved for the first time in ternary chromium sulfides, which adopt 1−3 dimensional frameworks of Cr-centered polyhedra.

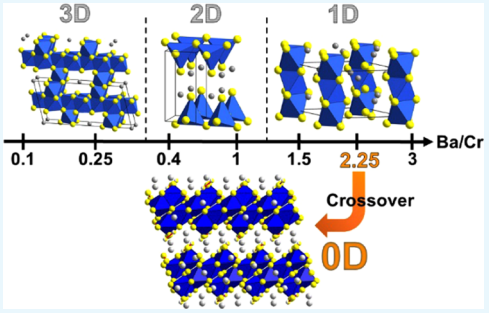

INTRODUCTION

Polysulfide compounds with S−S bonds or S_n^{2-} ($2 \leq n$) anions are of great interest because they can be used in a wide range of practical applications, for example, rechargeable alkali ion batteries,[1] vulcanized rubber,[2] and hydrodesulfurization catalysts.[3] The fundamental chemistry underlying such applications is the facile ability of sulfides to form or break covalent S−S bonds in specific reaction environments. However, in contrast to a large number of reports on glasses, complexes, and organometallics with polysulfide anions,[4−6] very few studies have been conducted on metal polychalcogenide solids because the low thermal stability of S_n^{2-} fragments (typically lower than 500 °C) is incompatible with high-temperature solid-state reactions required to obtain solid-state phases.[7]

Molten salt (flux) synthesis is one of the most useful approaches to obtain new extended solid-state polysulfide compounds.[7] Previous studies on polysulfide synthesis often used alkali-metal polysulfides with melting points much lower than 500 °C as flux, yielding novel polysulfides, mainly with d^0 and d^{10} transition metal cations (e.g., Ti^{4+}, Nb^{5+}, Cu^+, and Ag^+)[8−12] and main group metal cations (e.g., Te^{4+} and Sn^{2+}).[11,13] These polysulfides exhibit diverse low-dimensional frameworks in which the metal centers are anisotropically connected via bridging and/or chelating S_n^{2-} ligands. The S_n^{2-} fragments could be used as building blocks to design new low-dimensional magnetic/electrical materials. However, ternary or multinary polysulfide compounds with nonpaired electrons (i.e., d^1−d^9 metals) that show magnetism and electrical conductivity have not been sufficiently explored yet,[14,15] probably because of the high thermodynamic stability of simple binary metal sulfides.

A chromium sulfide system prefers to take oxidation states of chromium between +2 and +4. Although there are two binary chromium disulfides, namely, amorphous and crystalline CrS_3, ternary or multinary Cr-based polysulfides have never been reported. In the chromium sulfide system, ternary chromium sulfides have been the most extensively investigated because of their structural diversity.[16−19] In particular, the Ba−Cr−S system is the only one that shows a dimensional reduction of a Cr-based structural framework from three-dimensional (3D) (tunnel-like) through two-dimensional (2D) (layers) to one-dimensional (1D) (chains) units when the ratio of Ba/Cr atoms is increased (see Figure 1).[17,20,21] It should be noted that only high-pressure methods can access the infinite 1D chains of face-sharing CrS_6 octahedra as observed in Ba_3CrS_5 and $Ba_3Cr_2S_6$. In contrast, shorter octahedral chains are

Received: December 10, 2020
Accepted: February 17, 2021
Published: March 5, 2021

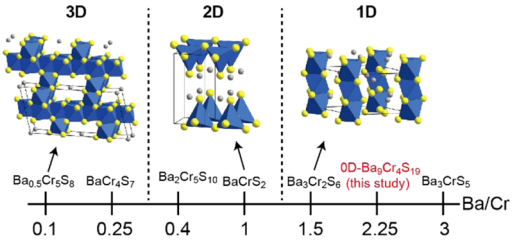

Figure 1. Relationship between the low-dimensional framework of Cr-centered polyhedra and the molar ratio of Ba/Cr.

typically linked by other Cr-centered polyhedra to form a 3D framework.

This study reports the first ternary chromium disulfide $Ba_9Cr_4S_{19}$, which could be obtained by a flux crystal growth method using $BaCl_2$ molten salt. This new compound shows a unique zero-dimensional structure composed of Cr_4S_{15} tetramer units thanks to the incorporation of disulfide ions.

RESULTS AND DISCUSSION

A photograph of single crystals of $Ba_9Cr_4S_{19}$ is shown in Figure 2. The single-crystal structure analysis revealed that $Ba_9Cr_4S_{19}$

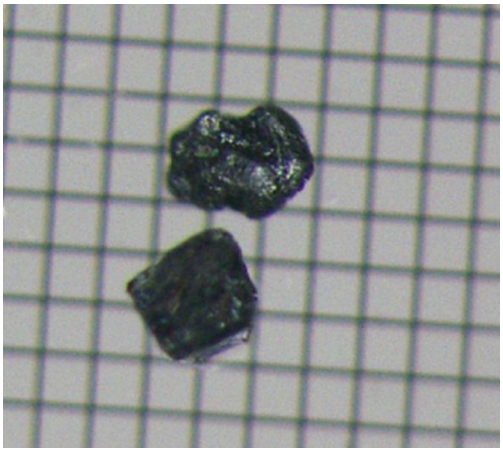

Figure 2. Photograph of single crystals of $Ba_9Cr_4S_{19}$ on a 1 mm grid-cell plate.

crystallizes in the space group $C2/c$ (No. 15) with the following unit cell parameters: a = 12.795(3) Å, b = 11.3269(2) Å, c = 23.2057(6) Å, β = 104.041(3) Å, and Z = 4. The details of the structure refinement are listed in Table 1, atomic coordinates and atomic displacement parameters are given in Table 2, and anisotropic displacement parameters are listed in Table S1. Selected bond distances and angles are summarized in Table S2. Solid-state reactions using a stoichiometric mixture of BaS, Cr_2S_3, and S were performed in an attempt to synthesize polycrystalline powder samples. Varying the reaction temperature and time did not yield the target phase at all; instead, unidentified phases were obtained. This result suggests that $BaCl_2$ flux is essential to obtain $Ba_9Cr_4S_{19}$.

Figure 3 shows the schematic view of the $Ba_9Cr_4S_{19}$ crystal structure along the b-axis and [301] directions. The present compound possesses a Cr_4S_{15} tetramer unit, half of which is an asymmetric unit because the middle point between two Cr1 atoms is positioned on a 2-fold axis (see Figure 4a). The four Cr-centered octahedra in the tetramer are linked by sharing the

Table 1. Results of the Structure Refinement of $Ba_9Cr_4S_{19}$ using Single-Crystal X-ray Diffraction Data

formula	$Ba_9Cr_4S_{19}$
formula weight	2053.11
radiation	Mo Kα (λ = 0.71073 Å)
T (K)	297
crystal system	monoclinic
space group	$C2/c$ (no. 15)
a (Å)	12.7695(3)
b (Å)	11.3269(2)
c (Å)	23.2057(6)
β (°)	104.041(3)
V (Å^3)	3256.16(13)
Z	4
D_{cal} (g/cm^3)	4.188
F_{000}	3616
no. of measured reflections	11 692
no. of unique reflections	3326
no. of observed reflections ($F^2 > 2\sigma(F^2)$)	2837
R_{int} (%)	2.89
final R_1/wR ($F^2 > 2\sigma(F^2)$) (%)	2.57/4.31
GoF	1.035
maximum/minimum residual peak (e/Å^3)	1.284/−1.093

common S_3 faces along the [301] direction. Two sulfur atoms, S6 and S7, bound to the Cr2 atom on each terminal face in the tetramer unit are coupled to each other at a bond distance of d_{S6-S7} = 2.0998(19) Å, in contrast to significantly longer distances between any other adjacent S−S bonds (~3.5 Å) in the Cr1/Cr2 octahedra. This short bond distance strongly suggests a dimerization of S6 and S7 atoms into a disulfide ion $(S_2)^{2-}$. In fact, the intramolecular distance is consistent with those typically observed in disulfide compounds.[22,23] Therefore, the terminal $Cr2(S_2)S_4$ octahedron is more distorted than the $Cr1S_6$ octahedron, which is also rationalized by a comparison of their distortion indices: D_{Cr1} = 0.01242 for $Cr1S_6$ and D_{Cr2} = 0.01648 for $Cr2(S_2)S_4$. Figure S1 shows the local coordination environment around Ba sites. These Ba atoms have 9- or 10-fold coordination for S atoms. In particular, Ba2, Ba3, and Ba5 are bound to disulfide ions (S9−S10, S9−S11, and S10−S11), which are described in detail below.

Each Cr_4S_{15} tetramer unit is separated via nonmagnetic Ba atoms in the ab plane so as to form a two-dimensional slab with four CrS_6 octahedral thickness, alternately stacked with a Ba_4S_4 (=$Ba_4(S_2)_2$) layer along the c-axis. As shown in Figure 4b, the four sulfur atoms (S9 × 2, S10, and S11) in the Ba_4S_4 layers form two types of disulfide ions (S9−S10 and S9−S11) along the [110] direction. The intramolecular bond distance between S9 and S11 (=1.892(4) Å) is shorter than that between S10 and S11 (=2.058(3) Å) atoms. The nearest inter-dimer S−S distance corresponding to d_{S9-S9} = 4.433(3) Å is significantly long, indicating a very weak interaction between the ions.

Considering the structure formed by disulfide ions, the chemical formula can be expressed as $Ba_9Cr_4(S_2)_4S_{11}$. Based on the charge balance, all chromium cations in $Ba_9Cr_4(S_2)_4S_{11}$ should be trivalent. The results of the bond valence sum (BVS) calculation are summarized in Table 3. The BVS values of Cr1 and Cr2 atoms are 2.83 and 2.946, respectively, which agree well with the expected ones. The BVS values of the S6, S7, S9, S10, and S11 atoms comprising disulfide ions are also

https://dx.doi.org/10.1021/acsomega.0c06017
ACS Omega 2021, 6, 6842−6847

Table 2. Crystallographic and Refinement Data Obtained from the Single-Crystal Structure Analysis of $Ba_9Cr_4S_{19}$

atom	site	x	y	z	occp.	U_{eq} ($10^2 \times Å^2$)
Ba1	8*f*	0.77471(2)	0.70539(3)	0.69208(2)	1	1.895(8)
Ba2	8f	0.38371(3)	0.67568(3)	0.56529(2)	1	2.190(9)
Ba3	8f	0.13367(2)	0.40518(3)	0.49137(2)	1	1.701(8)
Ba4	4e	0	0.35485(3)	3/4	1	1.162(9)
Ba5	8f	0.42825(3)	0.63735(3)	0.37094(2)	1	2.431(9)
Cr1	8f	0.38585(6)	0.52682(6)	0.71416(3)	1	0.936(17)
Cr2	8f	0.17169(6)	0.54902(6)	0.64108(3)	1	1.034(17)
S1	4e	1/2	0.34973(14)	3/4	1	1.21(4)
S2	8f	0.54271(9)	0.60900(10)	0.68742(5)	1	1.03(2)
S3	8f	0.28613(9)	0.70678(10)	0.68009(5)	1	1.33(3)
S4	8f	0.22482(9)	0.45936(10)	0.73887(6)	1	1.20(3)
S5	8f	0.31206(10)	0.43529(10)	0.61594(5)	1	1.24(3)
S6	8f	−0.00970(10)	0.59023(11)	0.65717(6)	1	1.70(3)
S7	8f	0.00784(10)	0.43141(11)	0.61379(6)	1	1.67(3)
S8	8f	0.12235(10)	0.65598(10)	0.54418(6)	1	1.39(3)
S9	8f	0.35172(17)	0.33883(15)	0.44804(9)	1	5.47(6)
S10	8f	0.4300(3)	0.4728(3)	0.48347(14)	0.5	3.11(7)
S11	8f	0.2824(2)	0.5016(2)	0.42524(14)	0.5	2.76(7)

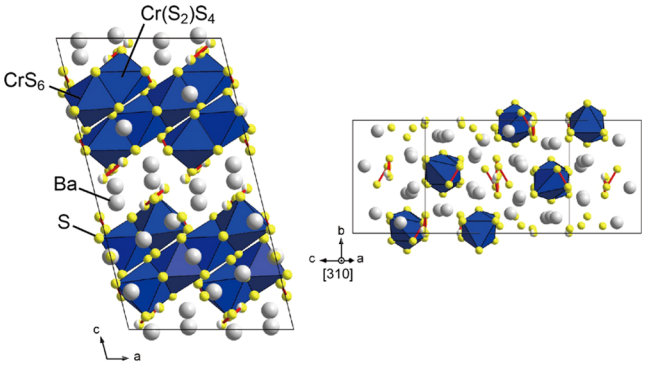

Figure 3. Crystal structure of $Ba_9Cr_4S_{19}$ viewed along the *b*-axis and [310] directions. Red bonds represent the dimerization of two sulfur atoms.

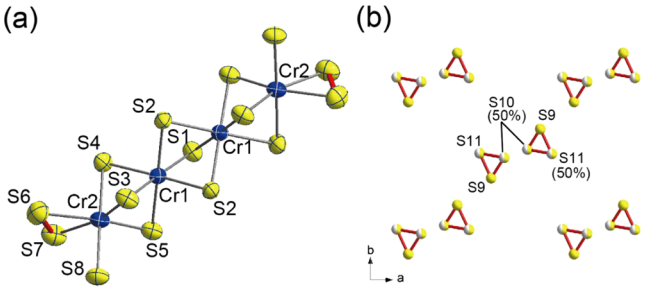

Figure 4. (a) Fragment of the Cr_4S_{15} tetramer unit. Displacement ellipsoids are shown at the 99% level. (b) Arrangement of disulfide ions in Ba_4S_4 layers on the *ab* plane. Half occupancy of S10 and S11 sites results in the formation of two independent disulfide ions, S9−S10 and S9−S11.

Table 3. Bond Valence Sum Values for $Ba_9Cr_4S_{19}$

atom	BVS	atom	BVS
Ba1	2.31	S1	−1.98
Ba2	2.27	S2	−2.33
Ba3	2.54	S3	−2.20
Ba4	2.55	S4	−2.07
Ba5	2.29	S5	−2.05
Cr1	2.95	S6	−1.19
Cr2	2.83	S7	−1.31
		S8	−1.98
		S9	−1.07
		S10	−0.74
		S11	−1.50

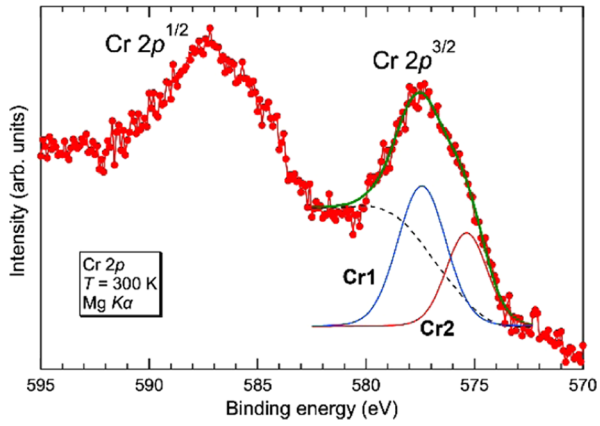

Figure 5. Cr 2p core-level photoemission spectrum collected from $Ba_9Cr_4S_{19}$ at 300 K. Blue and red lines represent the components derived from Cr1 and Cr2 sites, respectively. Bold green and dashed black lines represent the total fitting curve and the Shirley background, respectively.

consistent with the results of structural characterization. X-ray photoemission spectroscopy (XPS) measurements were performed to further investigate the oxidation states of these Cr ions. Figure 5 shows the Cr 2p XPS spectrum collected from single crystals of $Ba_9Cr_4(S_2)_4S_{11}$. The Cr $2p^{3/2}$ spectrum is decomposed into two components with binding energies of 575.37 and 577.43 eV, which could be assigned to Cr^{3+} species. The component at the lower binding energy should be assigned to the Cr2 atom bonded to a disulfide ion with an overall charge of −2.[24] The Cr1/Cr2 atomic ratio estimated from their spectral areas is 0.64:0.36, which roughly agrees with that obtained by structure analysis.

Both Cr1 and Cr2 atoms in a six-fold coordination form nonequivalent bonds with the surrounding sulfur ligands at

https://dx.doi.org/10.1021/acsomega.0c06017
ACS Omega 2021, 6, 6842−6847

distances ranging from 2.35 to 2.50 Å. These Cr−S bond distances are consistent with those in related ternary chromium sulfides with trivalent Cr ions, such as $Ba_3Cr_2S_6$[20] and $CsCr_5S_8$.[16] The Cr1−Cr1 and Cr1−Cr2 bond distances in the tetramer unit are 2.9854(14) and 2.8579(10) Å, respectively. Based on Pauling's third rule, a face-sharing octahedron is less stable than the corner- and edge-sharing ones because of the larger Coulomb repulsion between the neighboring cations in the former. The cation−cation distance between the ideal face-sharing octahedra can be described as $1.16 \times d_{Cr-S}$. Because the Cr-centered octahedra are distorted, the average bond distances of Cr1−(S1/S2/S2) and Cr1−(S3/S4/S5) were considered to roughly estimate the Cr−Cr distances expected from ideal face-sharing $(Cr1)_2S_9$ and $(Cr1)(Cr2)S_9$ octahedra, respectively. As a result, the bond distances of 2.843 Å for Cr1−Cr1 and 2.771 Å for Cr1−Cr2 were obtained. The corresponding experimental values are 5.0 and 1.3% larger than the calculated values. This bond elongation possibly results from the reduction in Coulomb repulsion between the Cr atoms. However, its degree is not very large compared with those observed with 1D sulfides Ba_3CrS_5 and $Ba_3Cr_2S_6$ with infinite 1D chains of face-sharing octahedra,[20] in which the Cr−Cr bond distances are more than 10% longer than those expected from the ideal octahedra.

Dimensional reduction is widely observed in other multinary chalcogenides.[25−27] For example, RE-Ga-S systems (RE: rare-earth metal) systematically decrease the dimensional framework composed of Ga-centered polyhedra from 2D to 0D with increasing the molar ratio of RE/Ga.[25] In contrast, the zero dimensionality of $Ba_9Cr_4S_{19}$ is not in line with the relationship between the low-dimensional framework and the molar ratio of Ba/Cr in the Ba−Cr−S system.[21] The molar ratio of Ba/Cr for $Ba_9Cr_4S_{19}$ is 2.25, which is within the regime for the 1D framework (Figure 1). It is likely that two types of the arrangement of disulfide ions play an important role in the crossover from 1D to 0D. In the first, two disulfide pairs are arranged in a 2D manner between the 2D slabs composed of Cr-based tetramer units. Such a low-dimensional arrangement of polysulfide ions interrupts direct linkage between the metal-centered polyhedra. Similar dimensional reduction induced by polysulfide ions is observed in di- or multinary (oxy-)polysulfide compounds (e.g., VS_4[28] and $Ba_{10}S(VO_3S)_6$[29]). In the second type, disulfide ions occur on the terminal Cr-centered octahedra in the tetramer units, which would cause the breaking of 1D chains into smaller fragments. However, a disulfide ion does not always function as a ligand that reduces the dimensionality. For example, the amorphous chromium sulfide CrS_3 $(=Cr(S_2)_{1.5})$ comprises 1D chains of trivalent Cr atoms surrounded by six sulfur atoms, all of which form disulfide ions.[30] The three sulfur atoms are shared between each neighboring Cr atom in a chain and one of them is coupled with a sulfur atom from another chain, resulting in a complex 3D framework. Therefore, the existence of non-magnetic Ba atoms, which break the linkages of Cr-centered octahedra, is essential for dimensional reduction.

At present, the low-dimensional magnetism of the Ba−Cr−S system has not been sufficiently investigated because it is difficult to obtain sufficient samples to measure physical properties.[20,21] Based on the structure analysis, the Cr_4S_{15} tetramer unit can be regarded as a spin tetramer with two types of nearest-neighbor interactions: J_1 for Cr1−Cr2 and J_2 for Cr1−Cr1. Figure 6 shows the temperature dependence of the magnetic susceptibility ($\chi = M/H$) of $Ba_9Cr_4S_{19}$ in a magnetic field of 10 kOe. The data were collected from several tiny single crystals, which were identified as the present phase by single-crystal X-ray diffraction (XRD). No significant difference was observed between the zero-field-cooled (ZFC) and field-cooled (FC) data. The $\chi(T)$ does not obey the Curie−Weiss law in the measured temperature range; instead, it monotonically decreases with the decrease of the temperature. The upturn observed below 40 K is probably due to impurity phases or defects in the lattice. A close inspection, however, detected a small kink at approximately 320 K, implying an antiferromagnetic ordering. Given the similar values of the Cr1−(Cr1/Cr2) bond angles (Table S3), both J_1 and J_2 are expected to be antiferromagnetic. In principle, the ideal spin tetramer model does not exhibit a long-range magnetic order regardless of the sign/magnitude of the intratetramer interactions.[31] If $Ba_9Cr_4S_{19}$ is magnetically ordered, additional terms such as interchain interactions and magnetic anisotropies should be taken into account to describe the magnetic behaviors. Higher-temperature data of $\chi(T)$, theoretical calculations, and neutron diffraction experiments would be needed in future research.

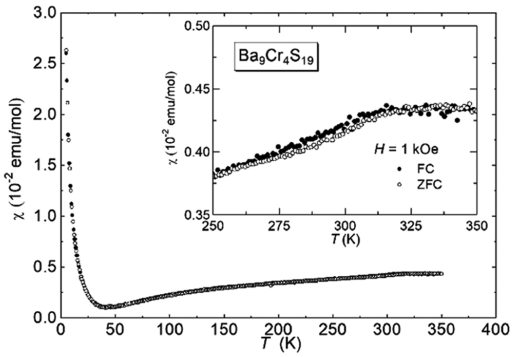

Figure 6. Temperature dependence of the magnetic susceptibility of $Ba_9Cr_4S_{19}$, measured under zero-field-cooled (ZFC) and FC conditions. The inset shows an enlarged view of the high-temperature data.

CONCLUSIONS

In conclusion, we have demonstrated the successful crystal growth of a new member of the Ba−Cr−S system, $Ba_9Cr_4S_{19}$, from $BaCl_2$ molten salt. The polysulfide ligands, which had never been formed in extended chromium sulfides, allowed access to the 0D framework of Cr-centered octahedra. The high-temperature flux method with non-sulfide molten salt shown in the present study opens up possibilities for obtaining novel low-D polysulfide magnets.

EXPERIMENTAL SECTION

Synthesis. $Ba_9Cr_4S_{19}$ single crystals were obtained by a flux crystal growth method using $BaCl_2$ molten salt. First, 0.875 mmol of BaS (High Purity Chemicals, 3N), 0.25 mmol of Cr_2S_3 (High Purity Chemicals, 3N), and 0.25 mmol of $BaCl_2$ (Rare Metallics, 3N) were thoroughly mixed, pelletized, and then loaded into an alumina crucible and sealed in a silica tube under vacuum. These starting materials were then heated in a muffle furnace to 1050 °C for 6 h, held for 24 h, cooled to 750 °C for 60 h, and then cooled to room temperature by turning the furnace off. To remove the flux and green powdery byproduct, the product was repeatedly washed with distilled water by sonication. Black block single crystals were collected

https://dx.doi.org/10.1021/acsomega.0c06017
ACS Omega 2021, 6, 6842−6847

via vacuum filtration. The typical dimensions of the $Ba_9Cr_4S_{19}$ single crystals were 0.2 × 0.2 × 0.05 mm^3.

Characterization. Structure determination of the single crystals was performed by a Rigaku XtaLab mini II diffractometer (Mo Kα radiation). The structure was solved by a dual-space algorithm method (*SHELXT*)[32] and refined by a full-matrix least-squares method with *SHELXL*,[33] using an Olex[2] graphical user interface.[34] X-ray photoemission spectroscopy (XPS) measurements were performed using a Mg Kα X-ray source (JEOL, JPS-9010MC). The Fermi level was calibrated using the C 1s signal. The magnetic susceptibility measurements were conducted in a magnetic field (H) of 1 kOe under zero-field-cooled (ZFC) and field-cooled (FC) conditions.

■ ASSOCIATED CONTENT

Supporting Information

The Supporting Information is available free of charge at https://pubs.acs.org/doi/10.1021/acsomega.0c06017.

Local coordination environment around Ba atoms; anisotropic displacement parameters; selected bond distances and bond angles; and crystallographic information (CIF)

Crystal structure; anisotropic displacement parameters; and bond distances and bond angles (PDF)

■ AUTHOR INFORMATION

Corresponding Author

Yoshihiro Tsujimoto − *International Center for Materials Nanoarchitechtonics (WPI-MANA), National Institute for Materials Science, Tsukuba, Ibaraki 305-0044, Japan; Graduate School of Chemical Sciences and Engineering, Hokkaido University, Sapporo 060-0808, Japan;* orcid.org/0000-0003-2140-3362; Email: TSUJIMOTO.Yoshihiro@nims.go.jp

Authors

Hong Yan − *International Center for Materials Nanoarchitechtonics (WPI-MANA), National Institute for Materials Science, Tsukuba, Ibaraki 305-0044, Japan; Graduate School of Chemical Sciences and Engineering, Hokkaido University, Sapporo 060-0808, Japan*

Yoshitaka Matsushita − *Materials Analysis Station, National Institute for Materials Science, Tsukuba 305-0047, Japan;* orcid.org/0000-0002-4968-8905

Akira Chikamatsu − *Department of Chemistry, The University of Tokyo, Tokyo 113-0033, Japan;* orcid.org/0000-0003-0484-6356

Tetsuya Hasegawa − *Department of Chemistry, The University of Tokyo, Tokyo 113-0033, Japan*

Kazunari Yamaura − *International Center for Materials Nanoarchitechtonics (WPI-MANA), National Institute for Materials Science, Tsukuba, Ibaraki 305-0044, Japan; Graduate School of Chemical Sciences and Engineering, Hokkaido University, Sapporo 060-0808, Japan;* orcid.org/0000-0003-0390-8244

Complete contact information is available at: https://pubs.acs.org/10.1021/acsomega.0c06017

Notes

The authors declare no competing financial interest.

■ ACKNOWLEDGMENTS

This work was supported by the JSPS KAKENHI (Grant Nos. 15H02024, 16H06438, 16H06441, 19H02594, 19H04711, 16H06439, and 20H05276) and a research grant from Innovative Science and Technology Initiative for Security, ATLA, Japan (No. JPJ004596).

■ REFERENCES

(1) Grayfer, E. D.; Pazhetnov, E. M.; Kozlova, M. N.; Artemkina, S. B.; Fedorov, V. E. Anionic Redox Chemistry in Polysulfide Electrode Materials for Rechargeable Batteries. *ChemSusChem* **2017**, *10*, 4805−4811.

(2) Uemura, S.; Matsuo, Y.; Okamatsu, T.; Arita, T.; Shimomura, M.; Hirai, Y. Low-Friction, Superhydrophobic, and Shape-Memory Vulcanized Rubber Microspiked Structures. *Adv. Eng. Mater.* **2020**, *22*, No. 1901226.

(3) Bej, S. K.; Maity, S. K.; Turaga, U. T. Search for an Efficient 4,6-DMDBT Hydrodesulfurization Catalyst: A Review of Recent Studies. *Energy Fuels* **2004**, *18*, 1227−1237.

(4) Draganjac, M.; Rauchfuss, T. B. Transition Metal Polysulfides: Coordination Compounds with Purely Inorganic Chelate Ligands. *Angew. Chem., Int. Ed.* **1985**, *24*, 742−757.

(5) Yu, X.; Manthiram, A. Highly Reversible Room-Temperature Sulfur/Long-Chain Sodium Polysulfide Batteries. *J. Phys. Chem. Lett.* **2014**, *5*, 1943−1947.

(6) Steudel, R.; Chivers, T. The Role of Polysulfide Dianions and Radical Anions in the Chemical, Physical and Biological Sciences, Including Sulfur-Based Batteries. *Chem. Soc. Rev.* **2019**, *48*, 3279−3319.

(7) Kanatzidis, M. G. Molten Alkali-Metal Polychalcogenides as Reagents and Solvents for the Synthesis of New Chalcogenide Materials. *Chem. Mater.* **1990**, *2*, 353−363.

(8) Sunshine, S. A.; Kang, D.; Ibers, J. A. A New Low-Temperature Route to Metal Polychalcogenides: Solid-State Synthesis of $K_4Ti_3S_{14}$, a Novel One-Dimensional Compound. *J. Am. Chem. Soc.* **1987**, *109*, 6202−6204.

(9) Burschka, C. Kristallstruktur von NH_4CuS_4/The Crystal Structure of NH_4CuS_4. *Z. Naturforsch., B* **1980**, *35*, 1511−1513.

(10) Bensch, W.; Dürichen, P. Preparation and Crystal Structure of the New Ternary Niobium Polysulfide K4Nb2S14 Exhibiting the Dimeric Complex Anion $[Nb_2S_{14}]_4$-. *Inorg. Chim. Acta* **1997**, *261*, 103−107.

(11) Nguyen, S. L.; Jang, J. I.; Ketterson, J. B.; Kanatzidis, M. G. $(Ag_2TeS_3)_2{\cdot}A_2S_6$ (A = Rb, Cs): Layers of Silver Thiotellurite Intergrown with Alkali-Metal Polysulfides. *Inorg. Chem.* **2010**, *49*, 9098−9100.

(12) Zhang, X.; Kanatzidis, M. G. $AMTeS_3$(A = K, Rb, Cs; M = Cu, Ag): A New Class of Compounds Based on a New Polychalcogenide Anion, TeS32-. *J. Am. Chem. Soc.* **1994**, *116*, 1890−1898.

(13) Liao, J. H.; Varotsis, C.; Kanatzidis, M. G. Syntheses, Structures, and Properties of Six Novel Alkali Metal Tin Sulfides: $K_2Sn_2S_8$, α-$Rb_2Sn_2S_8$, β-$Rb_2Sn_2S_8$, $K_2Sn_2S_5$, $Cs_2Sn_2S_6$, and Cs_2SnS_{14}. *Inorg. Chem.* **1993**, *32*, 2453−2462.

(14) Mizoguchi, H.; Gray, D.; Qiang Huang, F.; Ibers, J. A. Structures and Bonding in $K_{0.91}U_{1.79}S_6$ and KU_2Se_6. *Inorg. Chem.* **2006**, *45*, 3307−3311.

(15) Stüble, P.; Kägi, J. P.; Röhr, C. Synthesis, Crystal and Electronic Structure of the New Sodium Chain Sulfido Cobaltates(II), Na_3CoS_3 and $Na_5[CoS_2]_2(Br)$. *Z. Naturforsch., B* **2016**, *71*, 1177−1189.

(16) Huster, J. Darstellung Und Kristallstruktur Der Alkalithiochromate (III), ACr_5S_8 (A = Cs, Rb Und K). *Z. Anorg. Allg. Chem.* **1978**, *447*, 89−96.

(17) Petricek, S.; Boller, H.; Klepp, K. A Study of the Cation Order in Hollandite-like $M_xT_5S_8$ Phases☆. *Solid State Ionics* **1995**, *81*, 183−188.

(18) Rouxel, J.; Moëlo, Y.; Lafond, A.; DiSalvo, F. J.; Meerschaut, A.; Roesky, R. Role of Vacancies in Misfit Layered Compounds: The

Case of the Gadolinium Chromium Sulfide Compound. *Inorg. Chem.* **1994**, *33*, 3358−3363.
(19) Fuentes, O.; Zheng, C.; Check, C. E.; Zhang, J.; Chacon, G. Synthesis and Structural Analysis of $BaCrS_2$. *Inorg. Chem.* **1999**, *38*, 1889−1893.
(20) Fukuoka, H.; Miyaki, Y.; Yamanaka, S. High-Pressure Synthesis and Structures of Novel Chromium Sulfides, Ba_3CrS_5 and $Ba_3Cr_2S_6$ with One-Dimensional Chain Structures. *J. Solid State Chem.* **2003**, *176*, 206−212.
(21) Fukuoka, H.; Miyaki, Y.; Yamanaka, S. High-Pressure Synthesis and Structures of New Barium Chromium Sulfides, $BaCr_4S_7$ and $Ba_2Cr_5S_{10}$, with New Type Face-Sharing CrS_6 Structure Units. *Bull. Chem. Soc. Jpn.* **2007**, *80*, 2170−2176.
(22) Böttcher, P. Synthesis and Crystal Structure of the Dirubidiumpentachalcogenides Rb_2S_5 and Rb_2Se_5. *Z. Kristallogr. - Cryst. Mater.* **1979**, *150*, 1−4.
(23) Tegman, R. The Crystal Structure of Sodium Tetrasulphide, Na_2S_4. *Acta Crystallogr., Sect. B: Struct. Sci., Cryst. Eng. Mater.* **1973**, *29*, 1463−1469.
(24) Xi, K.; He, D.; Harris, C.; Wang, Y.; Lai, C.; Li, H.; Coxon, P. R.; Ding, S.; Wang, C.; Kumar, R. V. Enhanced Sulfur Transformation by Multifunctional FeS_2/FeS/S Composites for High-Volumetric Capacity Cathodes in Lithium-Sulfur Batteries. *Adv Sci* **2019**, *6*, No. 1800815.
(25) Lin, H.; Shen, J.; Zhu, W.-W.; Liu, Y.; Wu, X.-T.; Zhu, Q.; Wu, L. Two New Phases in the Ternary RE−Ga−S Systems with the Unique Interlinkage of GaS 4 Building Units: Synthesis, Structure, and Properties. *Dalton Trans.* **2017**, *46*, 13731−13738.
(26) Lin, H.; Shen, J. N.; Shi, Y. F.; Li, L. H.; Chen, L. Quaternary Rare-Earth Selenides with Closed Cavities: $Cs[RE_9Mn_4Se_{18}]$ (RE = Ho-Lu). *Inorg. Chem. Front.* **2015**, *2*, 298−305.
(27) Li, Y. Y.; Liu, P. F.; Lin, H.; Wu, L. M.; Wu, X. T.; Zhu, Q. L. Quaternary Semiconductor $Ba_8Zn_4Ga_2S_{15}$ Featuring Unique One-Dimensional Chains and Exhibiting Desirable Yellow Emission. *Chem. Commun.* **2019**, *55*, 7942−7945.
(28) Allmann, R.; Baumann, I.; Kutoglu, A.; Rösch, H.; Hellner, E. Die Kristallstruktur Des Patronits $V(S_2)_2$. *Naturwissenschaften* **1964**, *51*, 263−264.
(29) Nicoud, S.; Mentré, O.; Kabbour, H. The $Ba_{10}S(VO_3S)_6$ Oxysulfide: One-Dimensional Structure and Mixed Anion Chemical Bonding. *Inorg. Chem.* **2019**, *58*, 1349−1357.
(30) Hibble, S. J.; Walton, R. I.; Pickup, D. M. Local Structures of the Amorphous Chromium Sulfide, CrS_3, and Selenide, $CrSe_3$, from X-Ray Absorption Studies. *J. Chem. Soc., Dalton Trans.* **1996**, *11*, 2245−2251.
(31) Bonner, J. C.; Kobayashi, H.; Tsujikawa, I.; Nakamura, Y.; Friedberg, S. A. Theoretical Studies on the Isolated Spin Cluster Complex, Tetrameric Cobalt (II) Acetylacetonate $Co_4(C_5H_7O_2)_8$: Effects of Competing Superexchange Interactions. *J. Chem. Phys.* **1975**, *63*, 19−34.
(32) Sheldrick, G. M. SHELXT - Integrated Space-Group and Crystal-Structure Determination. *Acta Crystallogr., Sect. A: Found. Adv.* **2015**, *71*, 3−8.
(33) Sheldrick, G. M. Crystal Structure Refinement with SHELXL. *Acta Crystallogr., Sect. C: Struct. Chem.* **2015**, *71*, 3−8.
(34) Dolomanov, O. V.; Blake, A. J.; Champness, N. R.; Schröder, M. OLEX: New Software for Visualization and Analysis of Extended Crystal Structures. *J. Appl. Crystallogr.* **2003**, *36*, 1283−1284.

https://dx.doi.org/10.1021/acsomega.0c06017
ACS Omega 2021, 6, 6842−6847